

Design and Analysis of Ultra Low-Profile ILA on a Rectangular Conducting Plane

Erfan Rohadi¹, Mochammad Firdaus Ali^{2*}, Indrazno Siradjuddin², Awan Setiawan², Amalia Amalia², Yudhi Darmawan²

¹State Polytechnic of Malang, Information Technology Department

²State Polytechnic of Malang, Electrical Engineering Department

Jl. Soekarno Hatta No. 9, 65141, Malang, Indonesia

*Corresponding author E-mail: mfirdaus@polinema.ac.id

Abstract

The unbalanced fed ultra low profile inverted L antenna on a rectangular conducting plane is proposed and analyzed numerically and experimentally. By adjusting the length and height of inverted L antenna, the feed point position, and the size of conducting plane, the return loss bandwidth and the directivity can be controlled. The return loss bandwidth of 2.57 % and the directivity of 4.34 dBi are obtained, when the size of conducting plane is 0.245λ (λ : wavelength) by 0.49λ , and the antenna height is $\lambda/30$. The input impedance of the proposed antenna is compared with those of the conventional base-fed inverted L antenna and the base fed inverted F antenna. Although the directivity of base-fed inverted L antenna is almost same as that of proposed antenna, its input resistance becomes very low. In the base fed inverted F antenna, the return loss larger than 10 dB is not satisfied in the case of the antenna height less than 0.05λ .

Keywords: ILA, Low Profile Antenna, Return Loss, Unbalanced Fed, WIPL-D.

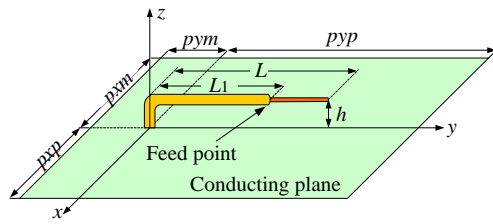
1. Introduction

The input impedance of horizontal dipole positioned very close to a perfect conducting plane becomes low due to the occurrence of a metallic structure, and it approaches zero as the distance decreases toward zero [1 - 3]. An ultra-low profile dipole antenna, which is a horizontal dipole very closely positioned to an infinite conducting plane was proposed to solve the impedance matching problem [4]. A half wave-length dipole is excited at the offset points from its center, so that reasonable impedance can be attained even with a conducting plane in proximity to the dipole. The maximum gain is higher than that of a half-wave dipole with a quarter wavelength distance between the dipole and the reflector about 8.4 dBi. The return loss bandwidth greater than 10 dB is about 2%. In order to realize ULPD, however, a 3 dB coupler and a 90° phase shifter are needed. The applied unbalanced feed by the author to the ultra low profile inverted L antenna positioned very close on a rectangular conducting plane and analyzed numerically and experimentally [5]. We may call this antenna as “ULPIL antenna” for convenience. As a low profile antenna, the base fed inverted F antenna is well known [6 - 11]. The antenna with base fed inverted F antenna in the case of the size of 0.245λ have been compared to 0.49λ [12]. In order to obtain the good return loss and the maximum directivity at the design frequency, many parameters such as the antenna height, the length of horizontal element, the feed point position and the size of conducting plane have to be optimized. In the previously reported references [5] and [12], the antenna parameters were not optimized.

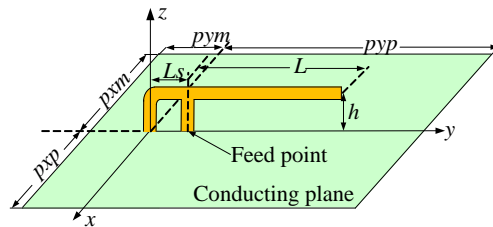
In this paper, the ULPIL antenna on a rectangular conducting plane is analysed numerically and experimentally and the relation between its characteristics and antenna parameters is discussed. The base fed inverted F antenna is compared by the characteristics of ULPIL antenna. In the numerical analysis, the electromagnetic for antenna simulator WIPL-D based on the Method of Moments is used [13].

2. Structure of proposed ULPIL antenna

Figure 1(a) shows the structure of the proposed antenna located on a rectangular conducting plane. The size of conducting plane is $p_x p_x + p_x m$ by $p_y p_y + p_y m$. The mounted semi-rigid coaxial cable with the characteristics impedance of 50Ω on the conducting plane. The radius of the outer conductor is 1.095 mm and that of the inner conductor is 0.255 mm, and PTEE (polytetrafluoroethylene) is filling the space within a coaxial cable [14]. This antenna consists of a horizontal arm in the y-direction and a small leg in the z-direction. The coaxial cable is extended behind ground plane. The generator is connected to the bottom end of coaxial cable. The inner conductor of the coaxial cable is extended from the end of outer conductor, that is, this antenna is excited at the end of outer conductor in the numerical analysis. The height of horizontal element is h . Figure 1(b) shows the conventional, base fed inverted F antenna. The design frequency is 2.45 GHz. The wavelength λ at 2.45 GHz is 122.45 mm. Since the edge singularity of electromagnetic field affects the antenna characteristics, the edge effect is considered in the numerical calculation [13].



(a) ULPIL antenna



(b) Base fed inverted F antenna

Fig. 1: ULPIL antenna and base fed inverted F antenna on a rectangular conducting plane.

3. Result and discussion

In this section, the relation between the return loss and directivity characteristics and the parameters of ULPIL antenna such as the antenna height h , the length of horizontal element L , the feed point position L_1 , the width of conducting plane $p_{xm} = p_{xp}$, the length between the base point of antenna and the end of conducting plane p_{yp} is discussed. The characteristics of ULPIL are also compared with those of the base fed inverted L antenna and the base fed inverted F antenna.

3.1 Effect of antenna height h

Table 1 shows the return loss bandwidth larger than 10 dB and the directivity for different antenna height h . The length of horizontal element L and the feed point position L_1 are optimized so that the resonant frequency becomes to be 2.45 GHz. The fixed antenna parameters are as follows; $p_{xp} = p_{xm} = 15$ mm, $p_{ym} = 10$ mm, $p_{yp} = 44$ mm. Figure 2 show the current distribution on ULPIL antenna for different h . As h becomes smaller the larger current flows on the conducting plane, since the mutual coupling between the inverted L antenna and the ground plane becomes stronger. Therefore the return loss bandwidth becomes narrower and the directivity becomes higher. When $h = 4$ mm ($\lambda/30$), the return loss bandwidth becomes 2.57 % and the directivity of 4.34 dBi is obtained. By adjusting the p_{yp} , the directivity becomes higher compared with the result of the reference [5].

Table 1: Return loss and directivity of ULPIL antenna for different antenna height h .

h	L	L_1	Return loss bandwidth			Directivity at 2.45GHz
			Lowest freq. [GHz]	Highest freq. [GHz]	[%]	[dBi]
2	31.8	26.9	2.439	2.459	0.82	4.79
4	31.0	22.6	2.417	2.480	2.57	4.34
6	29.8	18.2	2.392	2.509	4.78	4.18
8	28.3	14.2	2.386	2.545	6.49	4.01
10	26.8	9.9	2.334	2.581	10.08	3.81

$p_{xm} = p_{xp} = 15$ mm, $p_{ym} = 10$ mm, $p_{yp} = 44$ mm

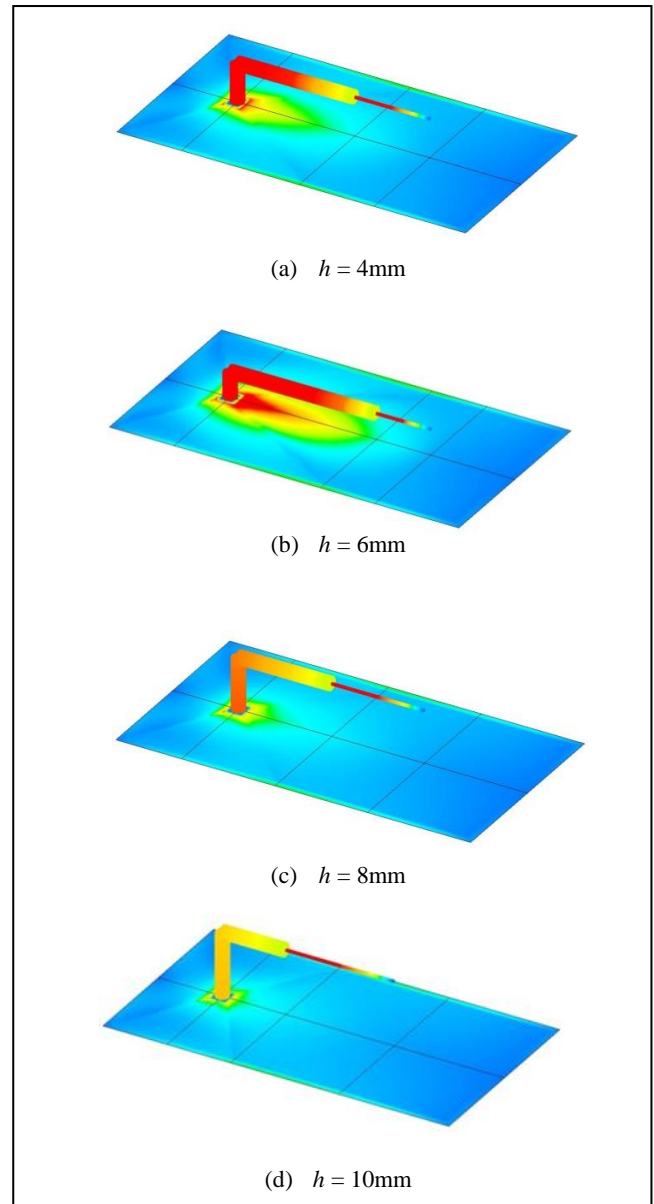


Fig. 2: Current distribution of ULPIL antenna. $p_{xm} = p_{xp} = 15$ mm, $p_{ym} = 10$ mm, $p_{yp} = 44$ mm.

3.2 Effect of length of horizontal element L

Figure 3 shows the input impedance characteristics of ULPIL for different L . $L_1 = 22.6$ mm, $h = 4$ mm, $p_{xm} = p_{xp} = 15$ mm, $p_{ym} = 10$ mm, and $p_{yp} = 44$ mm are fixed. In the case of $L = 31$ mm, the resonant frequency becomes to be 2.45 GHz. In the figure, the input impedances at the design frequency of 2.45 GHz are indicated by "x". When L is 30 mm, the input reactance becomes capacitive. On the other hand, when L is 32 mm, the input reactance becomes inductive. This is easily explained by the transmission line theory [15]. The input reactance of the open circuited parallel line becomes capacitive if its length becomes shorter than a quarter wavelength. Figure 4 shows the reflection coefficient for different L . L_1 is optimized so that the S_{11} becomes smallest at the resonant frequency in each case. The resonant frequencies in the case of $L = 30$ mm, 31 mm, and 32 mm are 2.535 GHz, 2.45 GHz, and 2.375 GHz, respectively. The length of L becomes almost a quarter wavelength at each resonant frequency. This means that the resonant frequency can be adjusted by L .

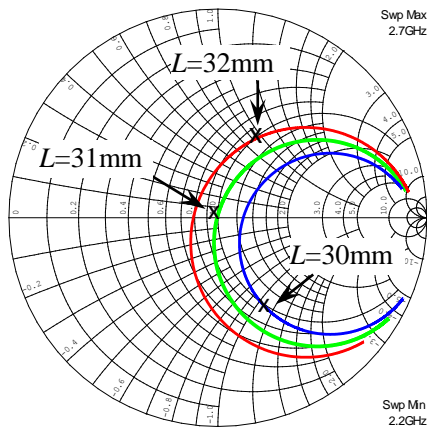


Fig. 3: Input impedance characteristics of ULPIL antenna for different L. $h = 4$ mm, $L_1 = 22.6$ mm, $p_{xm} = p_{xp} = 15$ mm, $p_{ym} = 10$ mm, $p_{yp} = 44$ mm.

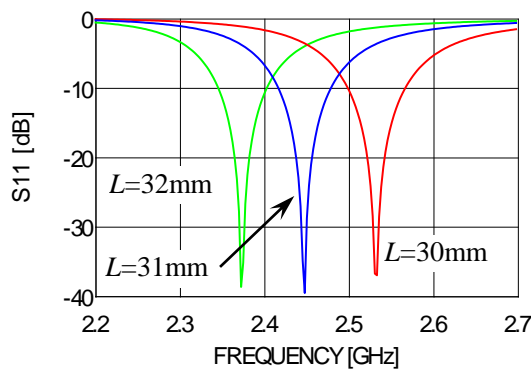
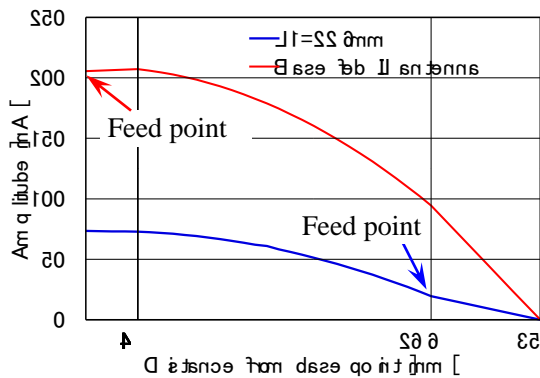


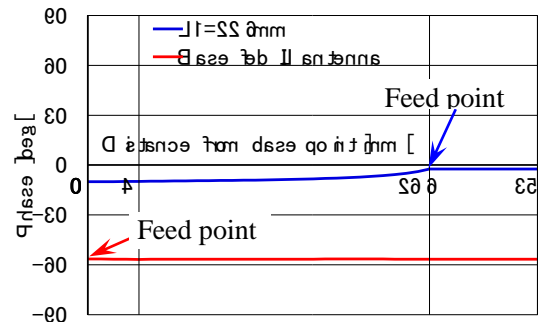
Fig. 4: S11 characteristics of ULPIL antenna for different L. L_1 is optimized. $h = 4$ mm, $p_{xm} = p_{xp} = 15$ mm, $p_{ym} = 10$ mm, $p_{yp} = 44$ mm.

3.3 Effect of feed point position L_1

Figure 5 shows the calculated current distributions of ULPIL with $L_1 = 22.6$ mm and the base fed inverted L antenna. The input impedance is defined by the ratio of the impressed voltage and the feed point current. Therefore the input resistance becomes smaller, as L_1 becomes smaller. The input impedance is 50Ω in the case of L_1 is 22.6 mm. That of base fed inverted L antenna is $4.06 + j26.85 \Omega$. The directivity of ULPIL with $L_1 = 22.6$ mm and the base fed inverted L antenna is 4.34 dBi and 4.86 dBi, respectively. Since the input impedance of the base fed inverted L antenna is mismatched to 50Ω , the actual gain of it becomes low.



(a) amplitude distribution



(b) Phase distribution

Fig. 5: Calculated current distribution at 2.45 GHz for different L_1 . $h = 4$ mm, $L = 31$ mm, $p_{xm} = p_{xp} = 15$ mm, $p_{ym} = 10$ mm, $p_{yp} = 44$ mm.

3.4 Effect of width of conducting plane $p_{xp} = p_{xm}$

Table 2 shows the return loss bandwidth and the directivity for different width of conducting plane $p_{xp} = p_{xm}$. The feed point position L_1 are optimized by the length of horizontal element L so that the resonant frequency becomes to be 2.45 GHz. As the width of conducting plane becomes wider up to 30 mm, the return loss bandwidth becomes narrower and the directivity becomes higher. The return loss bandwidth becomes wider and the directivity becomes lower following the changes width of the conducting plane becomes wider. In this antenna, as shown in Figure 2, the large current flows on the ground plane. This means that the current on the ground plane just under the horizontal element contributes to the radiation.

Table 2: Return loss and directivity of ULPIL antenna for different $p_{xp} = p_{xm}$

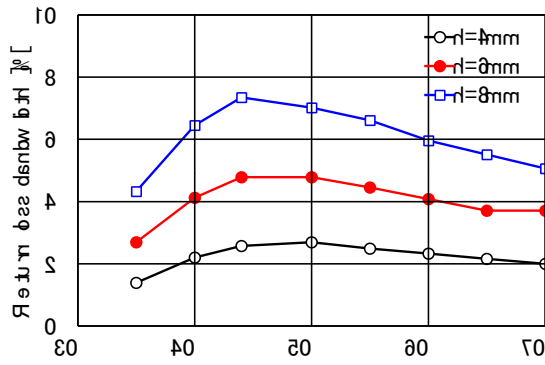
$p_{xp} = p_{xm}$ [mm]	L [mm]	L_1 [mm]	Return loss bandwidth			Directivity at 2.45GHz
			Lowest freq. [GHz]	Highest freq. [GHz]	[%]	[dBi]
10	31.9	20.9	2.392	2.504	4.57	4.17
15	31.0	22.6	2.417	2.480	2.57	4.34
20	30.6	23.2	2.426	2.473	1.92	4.40
25	30.4	23.5	2.432	2.471	1.59	4.48
30	30.3	23.7	2.432	2.468	1.47	4.51
35	30.1	23.5	2.432	2.469	1.51	4.47
40	30.1	23.4	2.432	2.47	1.55	4.26

$h = 4$ mm, $p_{ym} = 10$ mm, $p_{yp} = 44$ mm

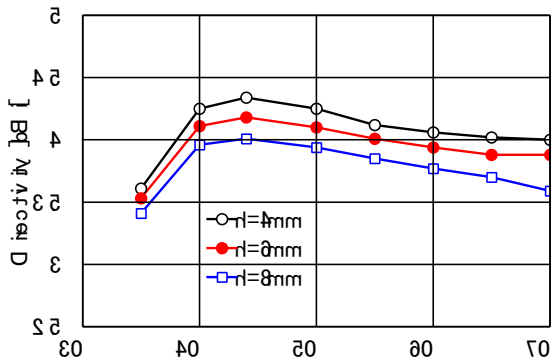
3.5 Effect of length of conducting plane p_{yp}

Figure 6 shows the return loss bandwidth and the directivity for different length p_{yp} between the base point of ULPIL and the end of conducting plane. $p_{xm} = p_{xp} = 15$ mm, and $p_{ym} = 10$ mm are fixed. The length L of horizontal element and the feed point position L_1 are optimized so that the resonant frequency becomes to be 2.45 GHz.

As the antenna height h becomes higher, the directivity becomes worse although the return loss bandwidth becomes wider. This may be due to the angle subtended at the ground plane by the horizontal element of inverted antenna becomes small as h becomes higher. When $p_{yp} = 44$ mm in the case of $h = 4$ mm, the directivity becomes maximum. Since the length of conducting plane becomes almost a half wavelength in this case, the large current flows on the conducting plane.



(a) Return loss bandwidth



(b) Directivity

Fig. 6: Return loss bandwidth and directivity of ULPIL antenna for different h . $p_{xm} = p_{xp} = 15$ mm, $p_{ym} = 10$ mm.

4. Comparison with base fed inverted F antenna

Table 3 shows the return loss bandwidth and the directivity of the base fed inverted F antenna for different antenna height h in the case of the length of short stub $L_s = 3.3$ mm. In this section, the dimension and parameters of conducting plane are fixed as $p_{xm} = p_{xp} = 15$ mm, $p_{ym} = 10$ mm, and $p_{yp} = 44$ mm. Table 4 shows the return loss bandwidth and the directivity of the base fed inverted F antenna for different length of short stub L_s . In both tables, L and L_1 are optimized so that the resonant frequency becomes to be 2.45 GHz. Figure 7 shows the input impedance characteristics of the base fed inverted F antenna for different h . In the base fed inverted F antenna, the input impedance is adjusted by changing the element length L and short stub length L_s . From Figure 7, when the antenna height h is less than 7 mm, the return loss larger than 10dB is not satisfied even though the antenna length is adjusted. Figure 8 shows the input impedance characteristics of the base fed inverted F antenna for different L_s . Figure 8 indicates that the input impedance is not matched when the short stub length L_s becomes longer than 5 mm.

Figure 9 shows the comparison of the return loss bandwidth and the directivity between ULPIL antenna and the base fed inverted F antenna. When the height h of the base fed inverted F antenna is less than 7 mm (about 0.05 λ), the return loss bandwidth larger than 10 dB is not satisfied even though the short stub is adjusted. Therefore, in Figure 9, data are not shown in the case of h is less than 7 mm. Figure 9 indicates that ULPIL antenna is very low profile and has higher gain compared with the base fed inverted F antenna.

Table 3: Return loss and directivity of base fed inverted F antenna for different h .

L_s	h	L	Return loss bandwidth			Directivity at 2.45GHz
			Lowest freq. [GHz]	Highest freq. [GHz]	[%]	[dBi]
3.3	7	26.2	2.388	2.520	5.39	4.02
3.3	8	25.6	2.353	2.556	8.29	3.92
3.3	9	24.9	2.334	2.587	10.33	3.80
3.3	10	24.3	2.312	2.610	12.16	3.69

$p_{xm} = p_{xp} = 15$ mm, $p_{ym} = 10$ mm, $p_{yp} = 44$ mm

Table 4: Return loss and directivity of base fed inverted F antenna for different L_s .

L_s	h	L	Return loss bandwidth			Directivity at 2.45GHz
			Lowest freq. [GHz]	Highest freq. [GHz]	[%]	[dBi]
3.3	10	24.3	2.312	2.610	12.16	3.69
4.0	10	25.2	2.311	2.612	12.29	3.71
5.0	10	26.5	2.314	2.603	11.80	3.73
6.0	10	27.3	2.325	2.580	10.41	3.76

$p_{xm} = p_{xp} = 15$ mm, $p_{ym} = 10$ mm, $p_{yp} = 44$ mm

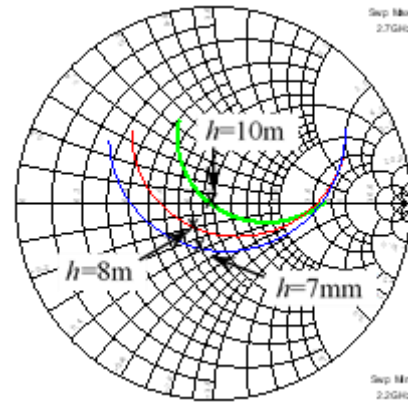


Fig. 7: Input impedance characteristics of base fed inverted F antenna for different h . $p_{xm} = p_{xp} = 15$ mm, $p_{ym} = 10$ mm, $p_{yp} = 44$ mm, $L_s = 3.3$ mm.

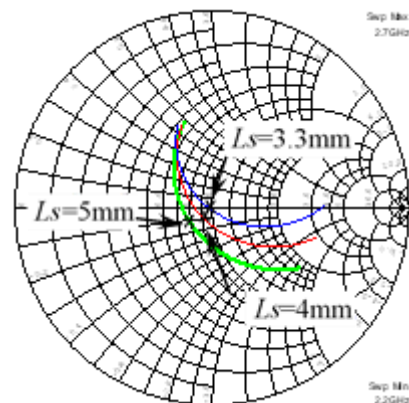
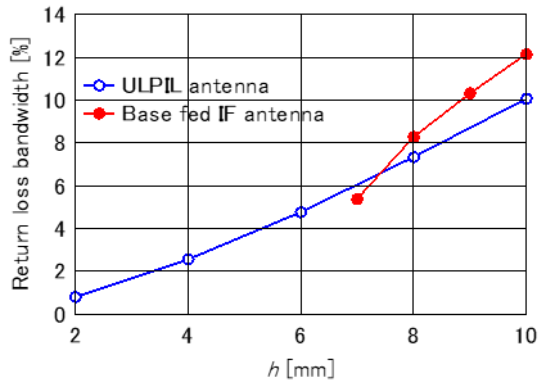
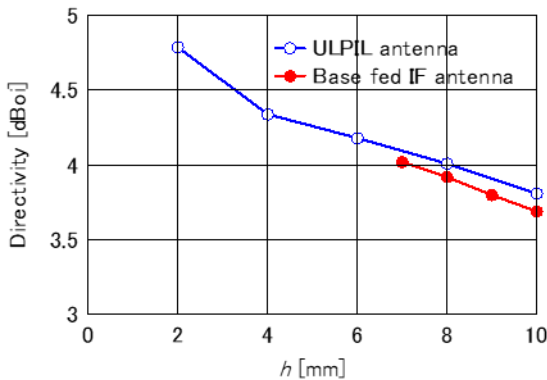


Fig. 8: Input impedance characteristics of base fed inverted F antenna for different L_s . $p_{xm} = p_{xp} = 15$ mm, $p_{ym} = 10$ mm, $p_{yp} = 44$ mm, $h = 10$ mm.



(a) Return loss bandwidth



(b) Directivity

Fig. 9: Comparison of return loss bandwidth and directivity between ULPIL antenna and base fed inverted F antenna. $p_{xm} = p_{xp} = 15$ mm, $p_{ym} = 10$ mm, $p_{yp} = 44$ mm, $L_s = 3.3$ mm.

5. Comparison with measurement

ULPIL antenna is fabricated and measured. Figure 10 shows the photograph of fabricated antenna [5]. The antenna parameters are as follows; $h = 4$ mm, $L = 31.1$ mm, $L_1 = 22.6$ mm, $p_{xp} = p_{xm} = 15$ mm, $p_{ym} = 10$ mm, $p_{yp} = 50$ mm. Figure 11 shows the calculated and measured return loss characteristics. The electric field radiation patterns at the frequency of 2.45 GHz shown in Figure 12. In the case of an antenna on a small conducting plane, the leakage current may flow on the coaxial cable behind the conducting plane. In order to evaluate the influence of the leakage current on the coaxial cable behind the conducting plane to the radiation pattern, the clamp filter composed of the ferrite core is attached on the coaxial cable behind the ground plane [16]. Figure 13 shows the measured electric field radiation patterns of the antenna with the clamp filter at the frequency of 2.45 GHz. From Figure 12, the measured radiation pattern is slightly different with the calculated pattern in the backward direction. This difference becomes small when the clamp filter is attached on the coaxial cable. Therefore the leakage current on the coaxial cable may be small although the ground plane is small compared with the wavelength.

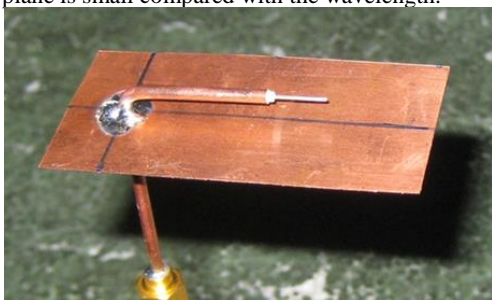


Fig. 10: Fabricated antenna.

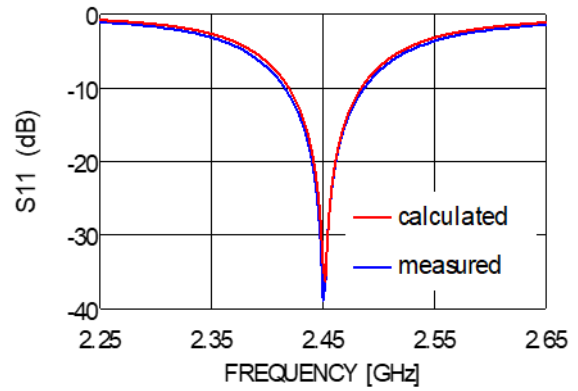


Fig. 11: Return loss characteristics of antenna. $h = 4.0$ mm, $L = 31.1$ mm, $L_1 = 22.6$ mm, $p_{xp} = p_{xm} = 15$ mm, $p_{ym} = 10$ mm, $p_{yp} = 50$ mm.

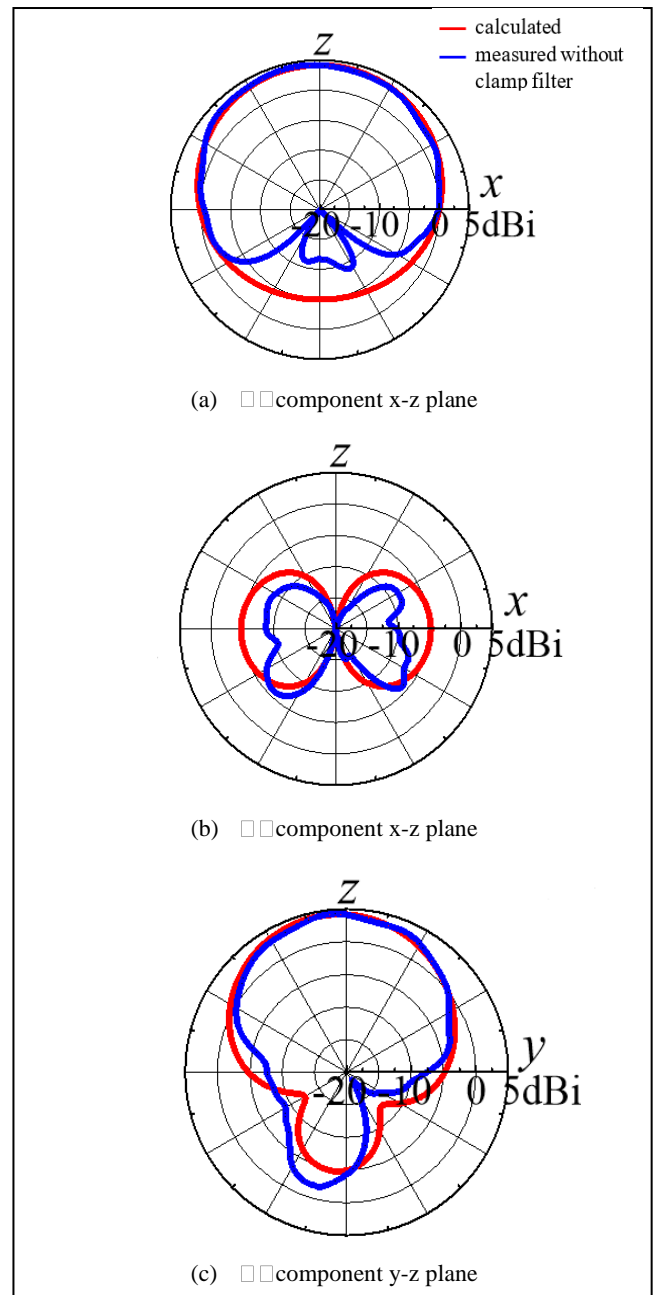


Fig. 12: Electric field radiation patterns of ULPIL antenna at 2.45GHz. $h = 4.0$ mm, $L = 31.1$ mm, $L_1 = 22.6$ mm, $p_{xp} = p_{xm} = 15$ mm, $p_{ym} = 10$ mm, $p_{yp} = 50$ mm.

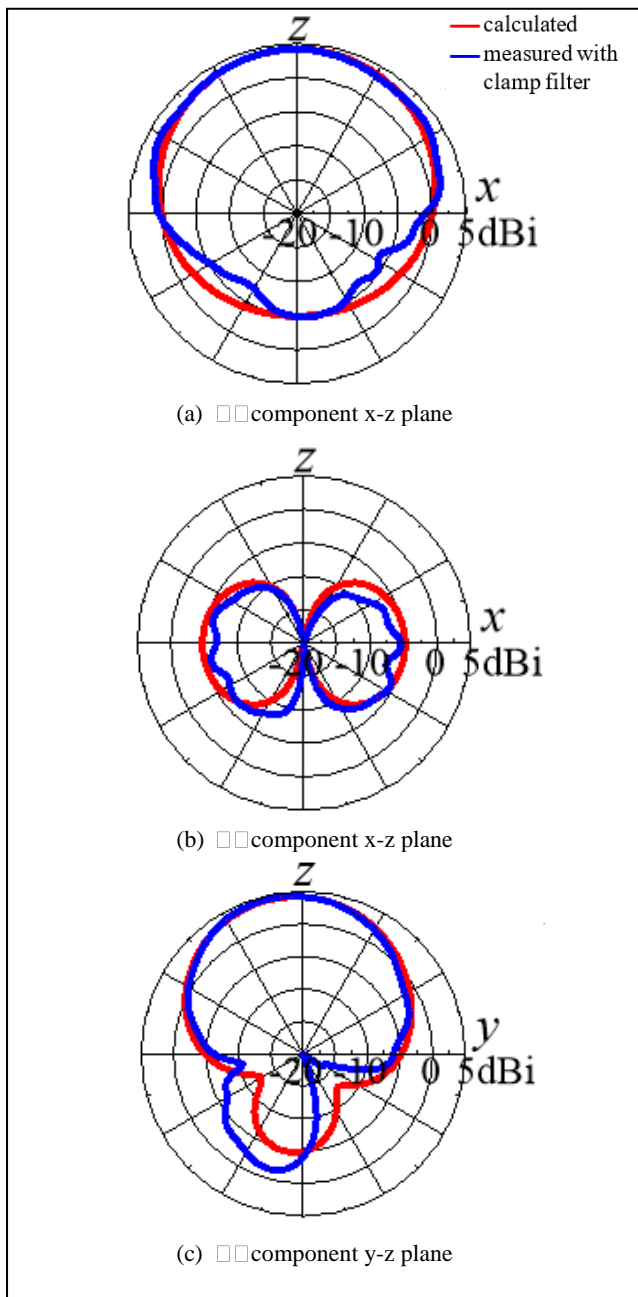


Fig. 13: Electric field radiation patterns of ULPIL antenna at 2.45GHz. $h = 4.0$ mm, $L = 31.1$ mm, $L_1 = 22.6$ mm, $p_x p = p_x m = 15$ mm, $p_y m = 10$ mm, $p_y p = 50$ mm.

6. Conclusion

The proposed and analyzed ultra-low profile unbalanced-fed inverted L antenna on the rectangular conducting plane resonant frequency is decided by the length of the horizontal element and the impedance matching can be done by adjusting the position of the feed point. The return loss bandwidth and the directivity are controlled by changing the antenna height and the size of rectangular conducting plane. When the size of conducting plane is 0.245λ by 0.45λ and the antenna height is $\lambda/30$, the return loss bandwidth larger than 10 dB becomes 2.57 % and the directivity is 4.34 dBi. The radiation characteristics of the base-fed inverted L antenna are almost same as those of proposed ULPIL antenna although the input resistance of base fed inverted L antenna becomes small. In this paper, the input impedance characteristics of the base fed inverted F antenna is also compared with the proposed ULPIL antenna. In the base fed inverted F antenna, the input impedance is adjusted by changing the length of horizontal element and the short stub length. If the antenna height of base fed

inverted F antenna is smaller than 0.05λ , the return loss larger than 10 dB is not satisfied. The proposed ULPIL antenna has high gain even though the antenna height is less than 0.05λ . The proposed antenna is applicable for the antenna for mobile terminal of the wireless communication.

Acknowledgement

The authors would like to express special thanks of gratitude to State Polytechnic of Malang for supporting this research.

References

- [1] J. D. Kraus: Antennas. New York: McGraw-Hill, pp. 425–427 and 461–467, 1988.
- [2] C. A. Balanis: Antenna Theory Analysis and Design. New York: Wiley, pp. 175–180, 1997.
- [3] S. A. Schelkunoff and H. T. Friis: Antennas Theory and Practice. New York: Wiley, 1952.
- [4] A. Thumvicit, T. Takano and Y. Kamata: “Characteristics verification of a half-wave dipole very close to a conducting plane with excellent impedance matching”, IEEE Trans. on Antennas and Propagat., vol.55, no.1, pp.53–58, Jan.2007.
- [5] T. Yamashita and M. Taguchi: “Ultra Low Profile Inverted L Antenna on a Finite Conducting Plane”, Proc. 2009 International Symp. on Antennas and Propagation, pp.361–364, Oct.2009.
- [6] H. Attia, M. M. Bait-Suwailan and O. M. Ramahi, “Enhanced Gain Planar Inverted-F Antenna with Metamaterial Superstrate for UMTS Applications”, Proc. PIERS., Cambridge, USA, pp. 494–497, 2010.
- [7] Z. N. Chen, K. Hirasawa, “A New Inverted F Antenna with a Ring Dielectric Resonator”, IEEE Trans. On Vehicular Technology, Vol. 48, No. 4, pp. 1029–1032, 1999.
- [8] D. Liu and B. P. Gaucher, “The inverted-F antenna height effects on bandwidth”, Proc. IEEE Antenna Propag. Symp., Vol. 2A, pp. 367–370, 2005.
- [9] D. Liu and B. P. Gaucher, “A branched inverted-F antenna for dual band WLAN applications”, Proc. IEEE Int. Symp. Antenna Propagations, Vol.3, pp. 2263–2266, 2004.
- [10] S. Schulteis, C. Waldschmidt, C. Kuhnert and W. Wiesbeck, “Design of a Capacitively Loaded Inverted F Antenna for Wireless-LAN Applications”, Proc. International ITG-Conference on Antennas, 178:187–190, 2003.
- [11] K. Ito and T. Hose, “Study on the characteristics of planar inverted F antenna mounted in laptop computers for wireless LAN”, Proc. IEEE Int. Symp. Antennas Propag., Vol. 2, pp. 22–25, 2003.
- [12] E. Rohadi and M. Taguchi, “Ultra low profile antenna for 2.45 GHz wireless communication”, Proc. 2012 IEEE Int. Conf. on Communications, Network and Satellite, pp.103–107, 2012.
- [13] “WIPL-D Pro v7.0 3D Electromagnetic Solver Professional Edition User’s Manual”, WIPL-D, 2009.
- [14] <http://www.coax.co.jp/english/semi/219.html>
- [15] D. M. Pozar: “Microwave Engineering”, Chapter 3, Addison-Wesley Publishing Company, 1990.
- [16] http://www.tdk.co.jp/tefe02/e9a15_zcat.pdf.